

# Influence of Water Clustering on the Dynamics of Hydration Water at the Surface of a Lysozyme

Alla Oleinikova, Nikolai Smolin, and Ivan Brovchenko

Physical Chemistry Department, Dortmund University, Dortmund, Germany

**ABSTRACT** Dynamics of hydration water at the surface of a lysozyme molecule is studied by computer simulations at various hydration levels in relation with water clustering and percolation transition. Increase of the translational mobility of water molecules at the surface of a rigid lysozyme molecule upon hydration is governed by the water-water interactions. Lysozyme dynamics strongly affect translational motions of water and this dynamic coupling is maximal at hydration levels, corresponding to the formation of a spanning water network. Anomalous diffusion of hydration water does not depend on hydration level up to monolayer coverage and reflects spatial disorder. Rotational dynamics of water molecules show stretched exponential decay at low hydrations. With increasing hydration, we observe appearance of weakly bound water molecules with bulklike rotational dynamics, whose fraction achieves 20–25% at the percolation threshold.

## INTRODUCTION

Biological function is possible only in presence of water, which is important for conformational stability and dynamics of biomolecules (see (1–3) for recent reviews). Experimental studies of some biosystems show that their physiological activity (for example, metabolism in *Artemia* cysts (4) and in various seeds (5)) appears rapidly at some critical hydration level. Important functions of biomolecules, such as enzymatic activity of proteins (6–12), proton pumping activity of bacteriorhodopsin (13) and its photoisomerization (14,15), and formation of biologically relevant B-form of DNA (16), also appear or intensify drastically when water content achieves some minimal hydration level, characteristic for each system. Typically, this hydration level is below the monolayer coverage of a biosurface. For some systems (protein powders (17,18), components of seeds (19,20), yeast (21), *Artemia* cysts (22), purple membrane (23)), this hydration level was found experimentally close to the percolation threshold of water, which marks appearance of a large spanning hydrogen-bonded water network instead of an ensemble of small water clusters upon increasing hydration. In the low-hydrated systems, water is localized in the vicinity of a biosurface and, accordingly, its percolation transition has quasi-two-dimensional character (17,19,21,23–25).

Importance of hydration water for the dynamics and functions of biomolecules is also seen from the studies of hydrated biomolecules at low temperatures. In the narrow temperature interval from 200 to 230 K, dynamics of various hydrated biomolecules show qualitative change, which correlates with onset of their biochemical activity upon heating

(26,27). This transition is weakly sensitive to the biomolecular structure, requires some minimal amount of water (28–30), and may be strongly affected by the presence of cosolvents. These facts indicate that the temperature-induced dynamic transition of biomolecules is governed by hydration water (31–34). Drastic change of water dynamics at ~220–240 K occurs in a similar way in silica pores (35,36) and at the surfaces of biomolecules (37,38). This dynamic transition of hydration water may reflect the phase transition of water (39) to the more ordered liquid phase upon cooling.

There are two main ideas that explain crucial role of hydration water in biofunction: water works as a plasticizer, providing conformational dynamics of biomolecules, required for their function (40); and water is an effective transport medium in biosystems (charge transport (41,42), transport of metabolites (6), etc.). In the interval of hydrations, where a spanning water network appears and transforms to permanent, dynamic properties of a hydrated biosystem change drastically. The well-known example is a steplike change of the dielectric properties of biosystems at some critical hydration level (17,20,24,42–47). At approximately monolayer water coverage, dynamics of a biomolecule become qualitatively similar to the observed at full hydration (48,49).

Computer simulations may give insight into microscopic mechanisms behind the hydration induced dynamic transition and function of biomolecules by the analysis of the effect of increasing hydration level on various physical properties of hydrated biomolecule. Increase of the hydration level causes qualitative change of the cluster structure of hydration water (50–58). At low hydrations, only small hydrogen-bonded water clusters are present in the system. At high hydrations, biomolecule is homogeneously covered by a hydrogen-bonded water network. The transition between these two states is a percolation transition of hydration water. As biofunction appears upon increasing hydration in the vicinity of this percolation transition, dynamics of hydrated biomolecules should

Submitted March 12, 2007, and accepted for publication June 20, 2007.

Address reprint requests to I. V. Brovchenko, Tel.: 49-231-755-3942; E-mail: brov@heineken.chemie.uni-dortmund.de.

N. Smolin's present address is Department of Medicinal Chemistry, University of Washington, Seattle, WA 98195-7610.

Editor: John E. Straub.

be studied with respect to water clustering and percolation. Clearly, this assumes that percolation threshold of hydration water should be localized on the surface of a biomolecule studied.

Translational and rotational dynamics of water molecules are essentially faster than the slow conformational motions of biomolecules and, therefore, can be studied by simulations in more detail. There are striking correlations between the fast motions of biomolecules and their slow conformational changes upon increasing hydration (59,60). Due to the strong coupling of water and protein motions, change of water dynamics may give information about dynamics of a biomolecule. Previous studies of water dynamics at the surfaces of biomolecules indicate strong slowing down of rotational and translational movements with decreasing hydration level both in experiment (61–64) and simulations (65–68). However, the large intervals between the hydration levels studied does not allow establishing the laws, which describe the evolution of water dynamics with hydration. Besides, water dynamics was never analyzed with respect to the clustering and percolation transition of hydration water.

We analyze the dynamics of hydration water at the surface of a hydrated lysozyme molecule. The properties of this enzyme at various hydrations were studied extensively in experiments and simulations (8,9,17,18,24,42–49,59,69–75). At low hydrations and up to  $h \approx 0.07$  (g of water per g of protein) water molecules are adjusted mostly to the charge groups of lysozyme and most protein motions are frozen. Rotational dynamics of methyl groups is observed at very low hydration and it seems to be rather insensitive to the hydration level and temperature. With increasing hydration, water molecules hydrate the polar groups and form larger water clusters. At  $h \approx 0.15$  (17,18,24) a quasi-two-dimensional percolation transition of water occurs and a hydrogen-bonded water cluster spans the whole lysozyme powder. The water percolation transition enables the long-range proton movement along the percolative water network and coincides with the first appearance of the enzymatic activity of lysozyme (8,48,49). Increase of the proton conductivity above the percolation threshold follows the power law predicted by the percolation theory (17). Recent light and neutron scattering experiments show sharp steplike increase of the fast relaxation process at  $h$  between 0.1 and 0.15, which was attributed to the rattling of residues in the cages formed by their neighbors (59,75). It is not clear whether this effect is related to the water percolation transition at  $h \approx 0.15$  due to the large interval between the hydration levels studied. These experiments suggest that sharp increase of the fast conformational fluctuations activates large-scale slow protein motions, which correlate well with the enzymatic (catalytic) activity (8,48,49). Experimental studies of hydrated lysozyme powder (9,49) indicate another important hydration level  $h \sim 0.38$ , which is attributed to the complete monolayer coverage of each lysozyme molecule. Below this hydration level (at  $h \sim 0.25$ ) all lysozyme molecules are covered with water, but

water shells are shared between two or more lysozymes. Above the one monolayer coverage, the full internal motions of protein are recovered, although the characteristic timescales are slower than at the infinite dilution. Note, that qualitatively similar changes of lysozyme dynamics are observed when dehydration is achieved by substitution of water by cosolvents (30,73,76).

In this article, we study the translational and rotational motions of water molecules near the surface of lysozyme upon increasing hydration from approximately one-third to one monolayer coverage. Analysis of water dynamics is preceded by the analysis of water clustering and by the localization of the percolation threshold of hydration water. To elucidate the effect of the dynamical motions of a lysozyme molecule onto dynamical properties of hydration water, simulations were performed for the rigid (frozen) and flexible lysozyme molecules.

## METHODS

Hen egg-white lysozyme (77) is a small globular protein with 129 amino-acid residues and contains  $\alpha$ -helices and a triple-stranded  $\beta$ -sheet in two structural domains. Lysozyme molecule (molecular mass of  $\sim 14.5$  kDa) was modeled, using the crystallographic heavy atom coordinates from the Protein Data Bank (78) (entry 2LYM (79)) and AMBER force field (80), which treats all atoms, including hydrogens, explicitly. For the residues, we chose the charge states corresponding to pH 7. The total charge of  $+8e$  on the protein surface was then neutralized by a uniform distribution of the opposite charge between all protein atoms to make the system neutral (adding a charge of  $-8e/1960 \approx -0.004e$  to each atom of the lysozyme molecule). The TIP4P model (81) was used for water. A spherical cutoff at 9 Å was used for truncation of the nonbonded interaction terms and the particle-mesh Ewald (82) summation method was used for the calculation of the electrostatic interactions. Integration time steps of 2 fs were used.

A single rigid or flexible model lysozyme molecule was placed in the center of a cubic box (edge length 60 Å), and periodic boundary conditions were applied. Hydrated systems were prepared by random placing of  $N_w$  water molecules in the free space of the simulation box. The water molecules were equilibrated at constant temperature during 1 ns in the field of the protein atoms. The number of water molecules  $N_w$  varied from 200 to 600. Molecular dynamics simulations of the lysozyme + water systems were done in the constant-volume  $NVT$  canonical ensemble. The temperature of the system was kept at  $T = 300$  K using separate coupling of protein and solvent to external temperature baths (67). We used Berendsen thermostat (83) with a coupling time of 0.5 ps and Nosé-Hoover algorithms (84,85) with a coupling time of 2.5 ps. Water clustering was analyzed in both cases and no difference in the cluster structure was detected. Analysis of water clustering and percolation was performed as described in detail elsewhere (50–58). Water molecules belong to the same cluster if they are connected by a continuous path of hydrogen bonds. Two water molecules are considered as hydrogen-bonded when the distance between the oxygen atoms is  $< 3.5$  Å and the water-water pair interaction energy is  $< -2.4$  kcal/mol. Molecular dynamics runs during 14 ns were used to study the translational and rotational dynamics of hydration water. Dynamics of water molecules was studied by the analysis of the trajectories every 1.0 ps for translations and every 0.2 ps for rotations. The dynamic properties of water were monitored only for water molecules near the protein surface. To exclude the contribution arising from the water molecules in a vapor phase, dynamics were studied only for water molecules with oxygens closer than 7.5 Å to the nearest heavy atom of a lysozyme molecule.

## RESULTS

### Percolation transition of hydration water

Percolation threshold of hydration water may be estimated from the calculation of the probability  $P(S_{\max})$  that, in an arbitrarily chosen configuration, the largest cluster contains  $S_{\max}$  water molecules. The probability distributions  $P(S_{\max})$ , of the size  $S_{\max}$  of the largest water cluster obtained at various hydration levels, are shown in Fig. 1 for the case of a flexible lysozyme molecule. Right peak of the distribution  $P(S_{\max})$  corresponds to the spanning water cluster, which homogeneously covers the biomolecule (54). The left peak represents nonspanning largest water clusters and it dominates at low hydrations. Analysis of the distributions  $P(S_{\max})$  allows location of the middle point of the percolation transition, where the probability  $R$  to observe a spanning water cluster is 50%. At this particular hydration level, distribution  $P(S_{\max})$  has the lowest height and the largest width. Fig. 1 shows that hydration level  $N_w = 375$  is the closest to the midpoint of the percolation transition.

The probability distribution  $P(S_{\max})$  allows more accurate location of the midpoint of the percolation transition (52,56) using the value  $S_{\max}^t = 225$ , which approximately separates spanning and nonspanning largest clusters (Fig. 1, vertical dashed line). Assuming that all largest water clusters with the size exceeding  $S_{\max}^t$  are spanning, the probability  $R$  to find a spanning cluster may be calculated as the integral of  $P(S_{\max})$  over  $S_{\max} > S_{\max}^t$ . The spanning probability  $R$  obtained in such a way at various hydration levels is shown in the upper panel of Fig. 2. Fit of  $R(N_w)$  to sigmoid function yields the inflection point at  $N_w \approx 380$ . The width  $\Delta S_{\max}$  of the probability distribution  $P(S_{\max})$  was computed as  $\Delta S_{\max} = \sqrt{\langle (S_{\max} - S_{\max}^{\text{av}})^2 \rangle} / N_w$ . It shows a maximum close to the

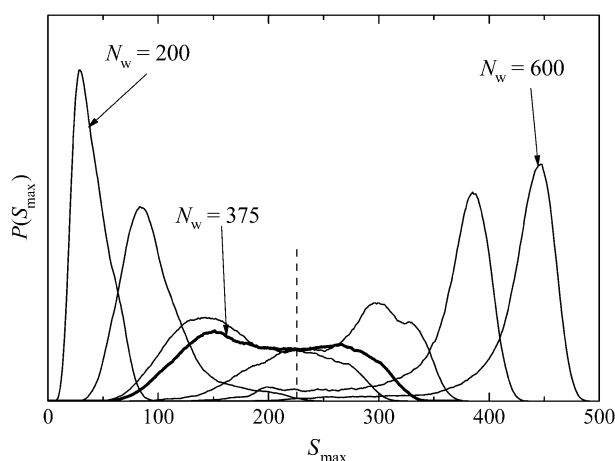


FIGURE 1 Size distribution  $P(S_{\max})$  of the largest water cluster at the surface of a flexible lysozyme molecule at various hydration levels:  $N_w = 200, 300, 350, 375, 400, 450, 500$ , and  $600$ . The distribution for  $N_w = 375$ , which is the closest to the midpoint of the percolation transition, is shown by the thick line. The vertical dashed line indicates  $S_{\max}^t = 225$ , which approximately separates spanning and nonspanning largest clusters.

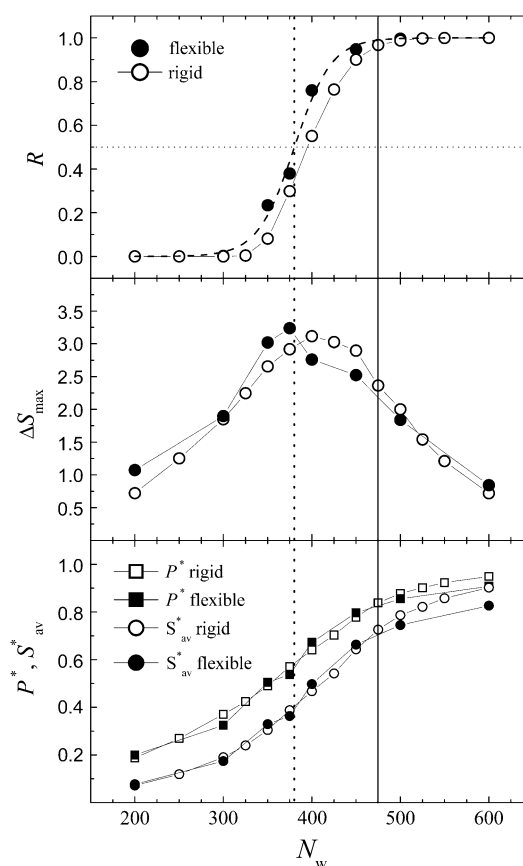


FIGURE 2 Spanning probability  $R$  (upper panel), width  $\Delta S_{\max}$  of the size distribution of the largest cluster (middle panel), fraction  $P^*$  of water molecules in the largest cluster, and the normalized average size  $S_{\text{av}}^*$  of water clusters (lower panel) at the surfaces of rigid and flexible lysozyme molecules at various hydration levels. The dashed line in the upper panel represents the fit of  $R$  for the flexible lysozyme to the sigmoid function with the inflection point at  $N_w \approx 380$  indicated by the vertical dotted line. True percolation threshold of water at the surface of the flexible lysozyme is shown by the vertical solid line.

inflection point of  $R(N_w)$ . This observation is also valid for the rigid lysozyme (middle panel in Fig. 2). The maximum of  $\Delta S_{\max}$  is observed at roughly the same hydration level as the maximum of the mean cluster size  $S_{\text{mean}} = \sum n_s S^2 / \sum n_s S$ , calculated without largest water cluster (56). The maximum of  $S_{\text{mean}}$  is located below the true percolation threshold in any finite system (86). Indeed, the percolation threshold of hydration water at  $N_w \approx 475$  was located from the cluster size distribution and fractal dimension of the largest water cluster at the surface of a rigid lysozyme (50). Fig. 2 shows that, for the flexible lysozyme, the percolation threshold slightly shifts to lower hydrations. This shift may be attributed to decrease of the water-accessible surface of a flexible lysozyme molecule relatively to a rigid lysozyme molecule.

In the lower panel of Fig. 2 we show fraction  $P^* = S_{\max} / N_w$  of water molecules belonging to the largest cluster, and

the normalized average size  $S_{av}^* = \sum n_S S^2 / N_w \sum n_S$  of all water clusters, including the largest one. Note that the function  $P^*$  is close to the well-known percolation probability  $P$  (fraction of molecules, belonging to the spanning cluster), when  $R$  approaches 1. The dependencies for rigid and flexible lysozyme molecules are rather similar. Note smaller size of the largest water cluster in the latter case for the high hydrations ( $N_w > 425$ ). This means that motions of lysozyme molecules cause some injuries to the spanning water clusters only.

### Translational dynamics of hydration water

The total (overall) mean-square displacement (MSD)  $\langle r^2 \rangle$  of water molecules at the surface of the rigid molecule was calculated for various times  $t$  as

$$\langle r^2 \rangle = \langle |\vec{r}_i(t) - \vec{r}_i(0)|^2 \rangle, \quad (1)$$

where average was taken over both the time origins and all water molecules in the hydration shell. In the case of a flexible lysozyme, MSD of water molecules was calculated relatively to the average coordinates of the backbone atoms and also in a laboratory system as for the rigid lysozyme molecule. The difference between  $\langle r^2 \rangle$  calculated by two methods was found negligible within accuracy of simulations, indicating a negligible displacement of the center of mass of the partially hydrated lysozyme molecule during the time interval of  $\sim 1$  ns when the MSD of each water molecule was calculated.

Time dependence of the total MSD of water at the surfaces of rigid and flexible lysozyme molecules are shown in Fig. 3 for some hydration levels. The value  $\langle r^2 \rangle$  continuously increases upon hydration. Similar behavior was observed in the simulation studies of water near the surface of differently hydrated plastocyanin (65,66). Translational mobility of water at the surface of a flexible lysozyme is noticeably higher than that at the surface of a rigid lysozyme. This difference is approximately a factor of two at low hydrations and it progressively vanishes at higher hydration levels. Considerable enhancement of water translational motion at low hydrations is obviously caused by the motions of the surface groups of a flexible lysozyme molecule. This effect diminishes at higher hydrations, when the role of water-water interactions in translational motion of water molecules becomes more important.

The time dependence of  $\langle r^2 \rangle$  is essentially nonlinear at all hydration levels studied. Such behavior is peculiar for confined systems and systems with temporal and spatial disorder. For example, in a cylindrical pore, MSD of molecules normally to the pore axis nonlinearly increases at short times and achieves saturation at longer times. As a result, the time dependence of the total MSD is nonlinear at short times and becomes linear only when displacements essentially exceed pore diameter. Due to the same reason,

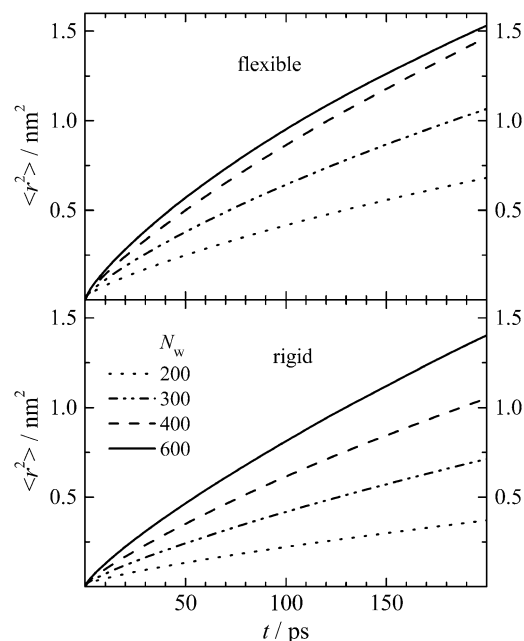


FIGURE 3 Total mean-square displacements  $\langle r^2 \rangle$  of water molecules at the surfaces of the flexible and rigid lysozyme molecules at various hydrations  $N_w$  shown in legend.

total MSD of water molecules adsorbed at the surface of a biomolecule (or the surface of any other finite object) cannot exceed some maximal value and achieves saturation at long times. At shorter times, when  $\sqrt{\langle r^2 \rangle}$  is essentially smaller than the size of a biomolecule,  $\langle r^2 \rangle$  varies with time  $t$  in accordance with a power law

$$\langle r^2 \rangle \sim t^\alpha, \quad (2)$$

where the exponent  $\alpha = 1$  for diffusion in homogeneous media (normal diffusion) and  $\alpha < 1$  for diffusion in inhomogeneous media (anomalous diffusion). Anomalous diffusion of water molecules at the surfaces of various biomolecules may originate from the roughness of the surface and from the strong spatial variations of the surface-water interaction and it was seen in some experiments and simulations (65,66,87,88).

For diffusion near a surface, it is reasonable to decompose the total MSD into the components parallel and perpendicular to the protein surface. For each time step, we have defined the distance of the molecule to the surface as a distance  $z$  from water oxygen to the nearest heavy atom of a lysozyme. The total displacement  $r$  was decomposed into displacement along  $z$  direction and displacement in  $xy$  plane, parallel to the surface of a lysozyme molecule (89). Note that such defined MSD  $\langle (xy)^2 \rangle$  characterizes diffusion of water along the lysozyme surface within some limited range of displacements only. Time dependences of  $\langle r^2 \rangle/3$ ,  $\langle (xy)^2 \rangle/2$ , and  $\langle z^2 \rangle$  for one of the studied system are shown in Fig. 4 (for other systems these dependencies look qualitatively

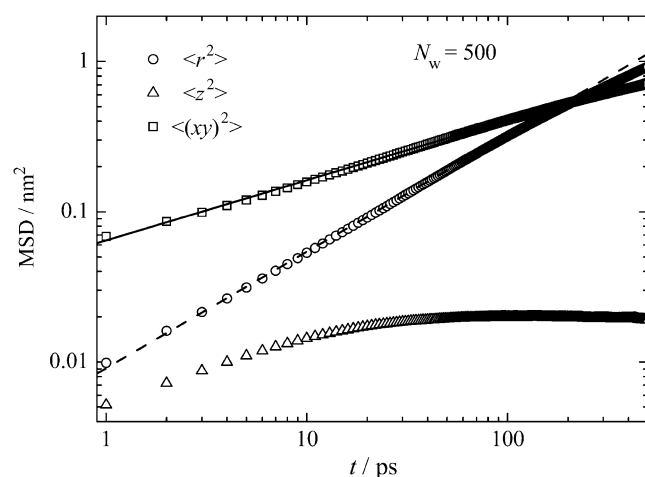


FIGURE 4 Time dependencies of the MSDs  $\langle r^2 \rangle/3$ ,  $\langle (xy)^2 \rangle/2$ , and  $\langle z^2 \rangle$  of water molecules at the surface of a flexible lysozyme molecule at  $N_w = 500$ . Solid and dashed lines show the time dependence  $\sim t^{0.40}$  and  $\sim t^{0.775}$ , respectively.

similar). As expected, MSD normal to the surface  $\langle z^2 \rangle$  achieves saturation rather quickly (at  $t < 100$  ps). The maximal MSD  $\langle z^2 \rangle$  reflects the average degree of the localization of water molecules in the vicinity of the lysozyme surface. The saturation value of  $\langle z^2 \rangle$  varies from  $\sim 0.01$  to  $0.02 \text{ nm}^2$  for both flexible and rigid lysozyme molecules in the hydration range studied. Both total MSD  $\langle r^2 \rangle$  and MSD  $\langle (xy)^2 \rangle$  parallel to the surface show anomalous diffusion.

The double-logarithmic plot of the time dependences of the total MSD  $\langle r^2 \rangle$  for water molecules at the surfaces of a flexible and rigid lysozyme molecules (Fig. 5) evidences that  $\langle r^2 \rangle$  follows Eq. 2 in a wide range of hydrations. In the time interval 10–100 ps the dependencies  $\langle r^2 \rangle(t)$  for  $N_w > 300$  may be well fitted to Eq. 2 with exponent  $\alpha = 0.775 \pm 0.010$  for the flexible lysozyme and  $\alpha = 0.793 \pm 0.010$  for the rigid lysozyme. The values of these exponents do not depend on the hydration level within the error bars shown. Independence of the obtained values of the exponent  $\alpha$  to hydration level indicates that the anomalous diffusion is caused mainly by the spatial disorder in the system. Noticeable deviations of  $\langle r^2 \rangle(t)$  from the Eq. 2 is seen at low hydrations, where effective value of  $\alpha$  continuously decreases at  $t < 10$  ps. These deviations should be attributed to the water molecules, which are strongly bound to lysozyme surfaces (there are  $\sim 36$  water molecules, having two or more hydrogen bonds with lysozyme molecule (45,46)). The total MSD of such water molecules quickly achieves saturation during their rather long residence times. So, our simulations indicate presence of two main classes of water molecules with respect to the translational motion: molecules with short residence times, which show anomalous diffusion due to the spatial disorder already at the short times; and molecules with long residence times, which remain bound to some centers at

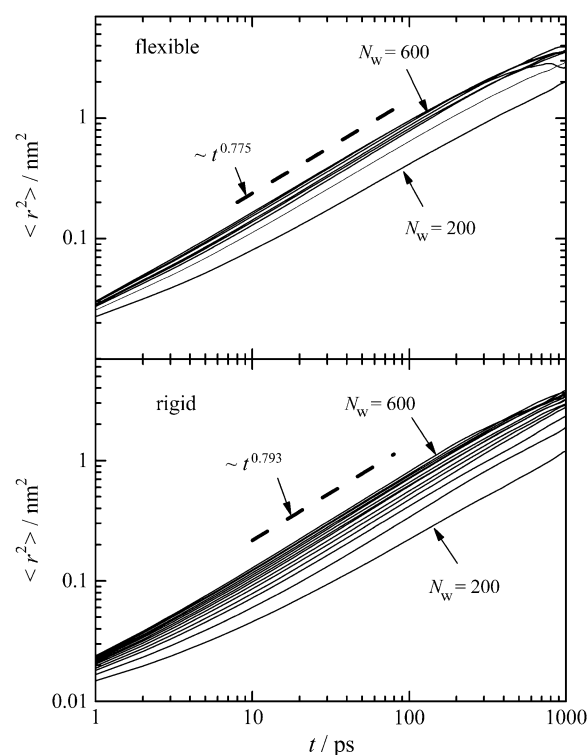


FIGURE 5 Time dependence of MSD  $\langle r^2 \rangle$  of water molecules at surfaces of the flexible and rigid lysozyme molecules in double logarithmic scale (solid lines). Hydration increases from the bottom to the top. The power laws corresponding to the anomalous diffusion (Eq. 2) with different values of  $\alpha$  are shown by dashed lines.

lysozyme surface during hundreds of picoseconds. Contribution of the latter molecules to the average MSD may be considered as a constant in the first approximation and the total MSD may be fitted to the equation

$$\langle r^2 \rangle \sim t^\alpha + \text{const.} \quad (3)$$

The time dependence of the total MSD was fitted to Eqs. 2 and 3 for each hydration level (Fig. 6). Clearly, Eq. 3 essentially better reproduces  $\langle r^2 \rangle(t)$  at short  $t$  for low hydrated systems. Relative contribution of the strongly bound water molecules to the total MSD decreases with increasing hydration level (compare the data for  $N_w = 200$  and  $N_w = 600$  in Fig. 6). When time  $t$  exceeds residence times of strongly bound water molecules, effect of spatial and temporal disorder cannot be distinguished and Eq. 2, with presumably lower value of the exponent  $\alpha$ , should be valid.

In case of anomalous diffusion, the dependence of the translational mobility of water on the hydration level can be characterized in different ways. We may compare the mean-square displacements  $\langle r^2 \rangle$  at some chosen time  $t$  or, alternatively, compare the times  $t$  yielding the same value of  $\langle r^2 \rangle$ . We may also characterize water mobility by the time-dependent effective diffusion coefficient  $D_{\text{eff}}(t)$ ,

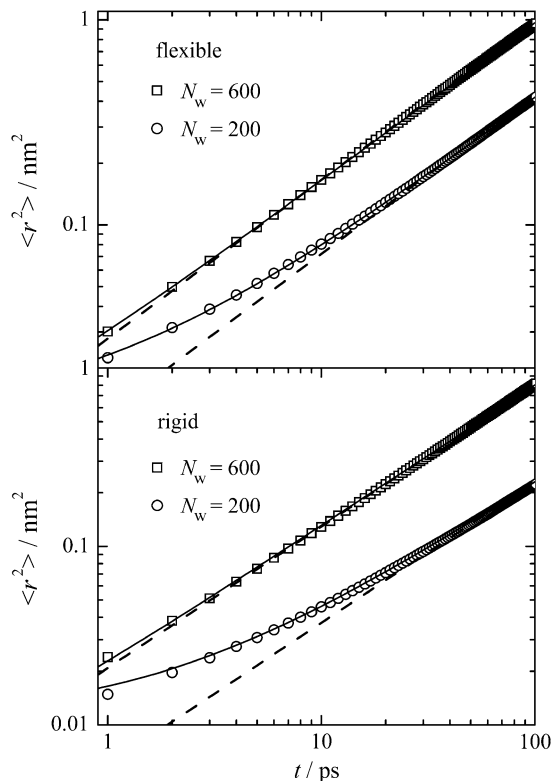


FIGURE 6 Time dependence of total MSD  $\langle r^2 \rangle$  of water molecules at surfaces of the flexible and rigid lysozyme molecules in double logarithmic scale. The fits to Eqs. 2 and 3 are shown by dashed and solid lines, respectively.

$$D_{\text{eff}} = \frac{\langle (r(t + \Delta t) - r(t))^2 \rangle}{2d\Delta t}, \quad (4)$$

where  $d$  is Euclidean dimension of a system ( $d = 3$  for the bulk water) and  $t \leq t + \Delta t$  is a time interval used for estimation.

Short-time water diffusion, which may be characterized by the total MSD  $\langle r^2 \rangle$  at  $t = 10$  ps, gradually increases with hydration level and tends to saturation just above the percolation threshold (see *upper left panel* in Fig. 7). The effective diffusion coefficients  $D_{\text{eff}}^{\text{tot}}$  and  $D_{\text{eff}}^{\parallel}$  were estimated by Eq. 4 for the total displacement  $\langle r^2 \rangle$  and for the displacement  $\langle (xy)^2 \rangle$  parallel to the surface, using  $d = 3$  and  $d = 2$ , respectively.  $D_{\text{eff}}^{\text{tot}}$  and  $D_{\text{eff}}^{\parallel}$ , calculated in the time interval  $5 \text{ ps} < t < 15 \text{ ps}$ , depend on hydration level similarly to  $\langle r^2 \rangle$  at  $t = 10$  ps (see *upper right panel* in Fig. 7). The values of  $D_{\text{eff}}^{\text{tot}}$  are noticeably lower than  $D_{\text{eff}}^{\parallel}$  due to the strong confining effect of a boundary on the displacement in  $z$  direction (normally to the surface). This effect is absent for the displacements parallel to the surface and  $D_{\text{eff}}^{\parallel}$  may be compared with the self-diffusion coefficient of bulk water  $D \approx 4.2 \times 10^{-9} \text{ m}^2 \text{ s}^{-1}$  for the water model studied (90) (see *horizontal line in the right upper panel* in Fig. 7). However, such comparison suffers from the fact that coefficient  $D_{\text{eff}}^{\parallel}$  is obtained from Eq. 4, which assumes linear time dependence

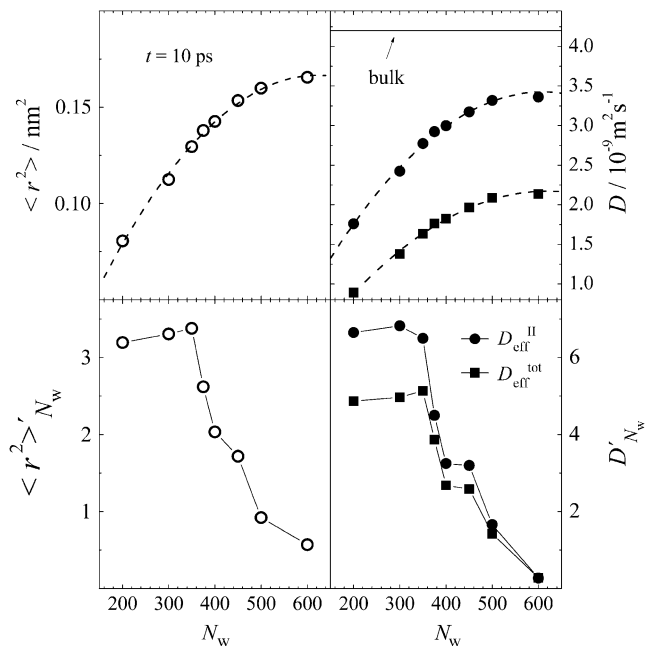


FIGURE 7 Total MSD  $\langle r^2 \rangle$  of water molecules at the surface of a flexible lysozyme molecule at  $t = 10$  ps (*left upper panel*) and its derivative with respect to  $N_w$  (*left lower panel*). Diffusion coefficients  $D_{\text{eff}}$  and  $D_{\text{eff}}^{\parallel}$  of water molecules at the surface of a flexible lysozyme molecule (*right upper panel*) and their derivatives with respect to  $N_w$  (*right lower panel*). Polynomial fits are shown by the dashed lines.

of MSD, whereas hydration water shows anomalous diffusion (see Figs. 5–7).

Dependence of water mobility on hydration may be further analyzed using the derivatives of  $\langle r^2 \rangle$ ,  $D_{\text{eff}}^{\text{tot}}$ , and  $D_{\text{eff}}^{\parallel}$  with respect to hydration level  $N_w$  (Fig. 7, *lower panels*). They show a rapid drop at the hydration level  $N_w \approx 380$ , corresponding to the midpoint of the percolation transition and approaches zero at the percolation threshold ( $N_w \approx 475$ ). Starting from the midpoint of the percolation transition, translational mobility of water correlates with the average size of water clusters, size of the maximal cluster, and spanning probability, which show roughly similar behavior in the considered range of hydrations (see Fig. 2). This correlation may be seen when water mobility is plotted as a function of the average cluster size  $S_{\text{av}}$ . For water at the surface of a flexible lysozyme, there is a linear correlation between mobility and  $S_{\text{av}}$  in a wide hydration range. For example, this correlation is seen when water mobility is characterized by the inverse time  $t^{-1}$  corresponding to the total MSD  $\langle r^2 \rangle = 0.1$  and  $\langle r^2 \rangle = 1 \text{ nm}^2$  (Fig. 8, *left panel*).

In the case of a rigid lysozyme, trend of water mobility to saturation with approaching the percolation threshold is much less pronounced (Fig. 9) and its correlation with cluster properties, such as  $S_{\text{av}}^*$ , is questionable (Fig. 8, *right panel*). This evidences importance of protein motions for mobility of hydration water. Obviously, the fast translational motions of water molecules should reflect mainly a local environment

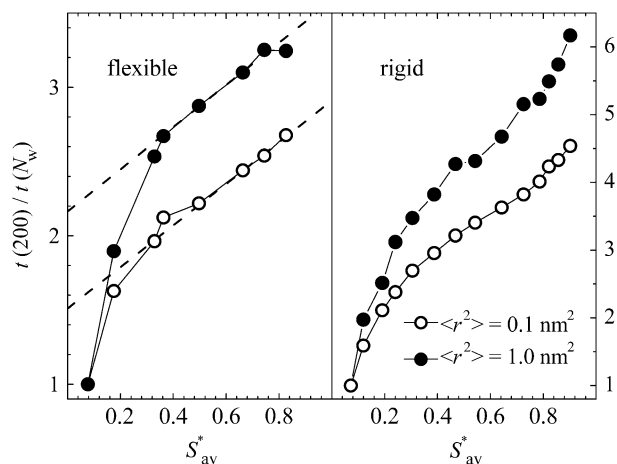


FIGURE 8 Normalized inverse time  $t(200)/t(N_w)$ , corresponding to the total MSD  $\langle r^2 \rangle = 0.1 \text{ nm}^2$  and  $\langle r^2 \rangle = 1.0 \text{ nm}^2$  of water molecules at the surface of the flexible and rigid lysozyme molecules as function of the normalized average cluster size  $S_{av}^*$ . Linear dependence is shown by dashed lines in the left panel.

of water molecule. This local environment may be divided on two parts, related to water-protein and water-water interactions. The latter part may be characterized, for example, by the average number  $n_H$  of H-bonded neighbors. Indeed, the short-time mobility of water at the surface of a flexible lysozyme, estimated in different ways, varies almost linearly with  $n_H$  in the whole hydration range studied (Fig. 10). Behavior of the short-range water mobility at the surface of a rigid lysozyme is qualitatively similar. However, contrary to the flexible lysozyme, the correlation between water mobility and  $n_H$  remains linear for larger displacements as well (Fig. 9, lower panel).

The coupling of water and lysozyme dynamics may be seen when the difference  $\Delta(t^{-1})$  between the mobilities of water at the surfaces of the flexible and rigid lysozyme molecules is considered (Fig. 11). This coupling is not sensitive to the time/length scale considered (compare *open* and *closed symbols* in Fig. 11). Clearly,  $\Delta(t^{-1})$  is the largest in the hydration range from  $N_w = 350$  to  $N_w = 500$ , where the probability  $R$  to observe a spanning water network varies from  $\sim 20$  to  $100\%$ .

### Rotational dynamics of hydration water

The rotational motion of water has been analyzed through the reorientational dynamics of its electrical dipole, defined as the vector pointing from the water oxygen to the middle point of the two hydrogen atoms. Two first- and second-rank autocorrelation functions  $\Gamma_1$  and  $\Gamma_2$  were calculated as the time average of the Legendre polynomials  $P_l(\cos(\theta))$ ,

$$\Gamma_1 = \langle P_1(t) \rangle = \langle \cos\theta(t) \rangle, \quad (5)$$

$$\Gamma_2 = \langle P_2(t) \rangle = \langle 3\cos^2\theta(t) - 1 \rangle, \quad (6)$$

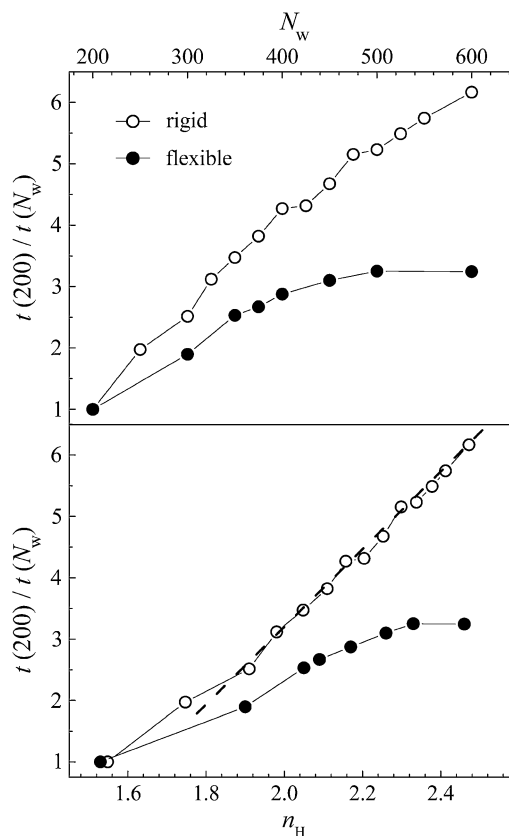


FIGURE 9 Normalized inverse time  $t(200)/t(N_w)$ , corresponding to the total MSD  $\langle r^2 \rangle = 1.0 \text{ nm}^2$  of water molecules at the surface of the flexible and rigid lysozyme molecules as function of the hydration level (*upper panel*) and of the average number  $n_H$  of H-bonded neighbors (*lower panel*). Linear dependence is shown by dashed line in the lower panel.

where  $\theta$  is the angle between dipole orientation at time  $t$  and its initial orientation. Both  $\Gamma_1$  and  $\Gamma_2$  decay faster toward zero at higher hydration levels.

At low hydrations, the decay of the autocorrelation function  $\Gamma_1$  may be described by the Kohlrausch-Williams-Watts stretched exponential equation (91,92):

$$\Gamma_1 = \exp\left(-\left(\frac{t}{\tau_1}\right)^\beta\right). \quad (7)$$

For example, time dependence of  $\Gamma_1$  for 200 water molecules at the surface of a flexible lysozyme may be well fitted by Eq. 7 with  $\beta = 0.325$  and  $\tau_1 \approx 48 \text{ ps}$  (see *upper dashed line* in Fig. 12). At higher hydration levels, decay of  $\Gamma_1$  cannot be described by one-term Eq. 7 (see *lower dashed line* in Fig. 12 for  $N_w = 600$ ). We have found at all hydrations studied that  $\Gamma_1$  may be well described by a two-terms equation, which includes, in addition to a stretched exponential, a simple Debye decay:

$$\Gamma_1 = (1 - a)\exp\left(-\left(\frac{t}{\tau_1}\right)^\beta\right) + a \exp\left(-\frac{t}{\tau_2}\right). \quad (8)$$

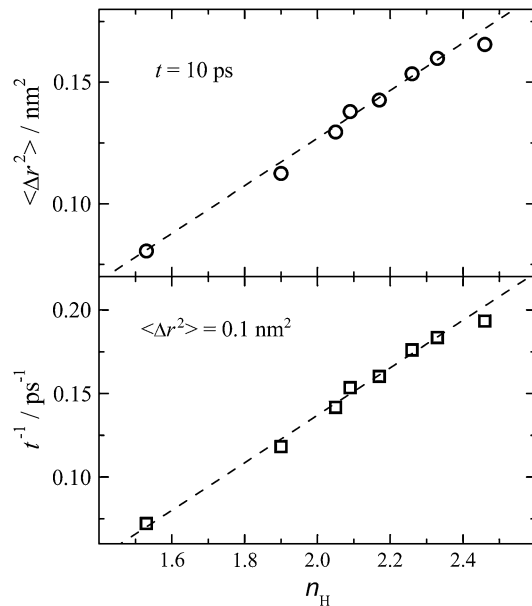


FIGURE 10 Total MSD  $\langle r^2 \rangle$  at  $t = 10$  ps (upper panel) and inverse time  $t^{-1}$ , corresponding to the total MSD  $\langle r^2 \rangle = 0.1 \text{ nm}^2$  (lower panel) of water molecules at the surface of a flexible lysozyme molecule as functions of the average number  $n_H$  of H-bonded neighbors. Linear fits are shown by dashed lines.

Equation 8 assumes an existence of two kinds of molecules, showing quite different reorientational dynamics in the considered time interval. Water molecules strongly bound to the lysozyme surface show stretched-exponential relaxation, whereas weakly bound molecules show simple one-term exponential relaxation, like in the bulk. Fractions of these two kinds of molecules,  $(1 - a)$  and  $a$ , respectively, should

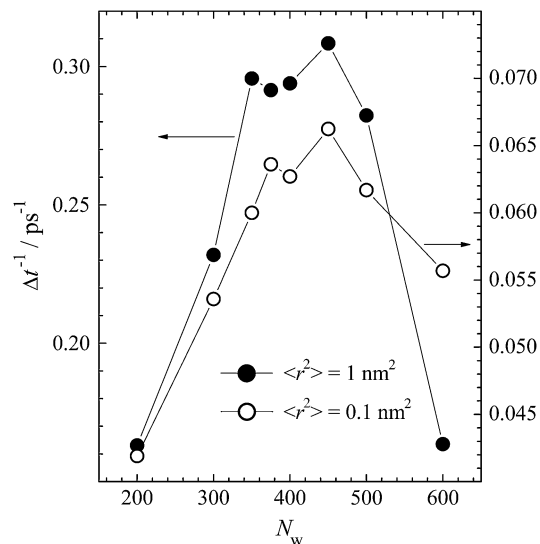


FIGURE 11 The difference  $\Delta t^{-1}$  between the inverse times, corresponding to the total MSD  $\langle r^2 \rangle = 0.1 \text{ nm}^2$  and  $\langle r^2 \rangle = 1.0 \text{ nm}^2$  of water molecules at the surfaces of flexible and rigid lysozyme molecules.

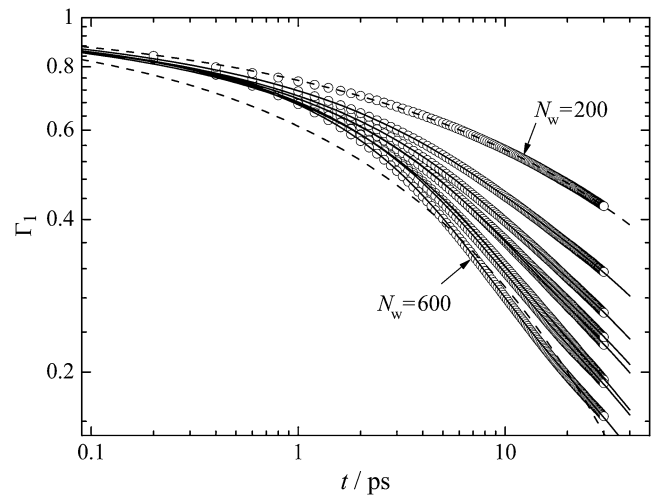


FIGURE 12 First-rank dipole-dipole autocorrelation function  $\Gamma_1$  of water at the surface of a flexible lysozyme at various hydrations  $N_w$ . The fits of stretched exponential Eq. 7 to  $\Gamma_1$  for the lowest and highest hydrations studied are shown by dashed lines. The fits of the data to the two-term Eq. 8 are shown by solid lines.

depend on the hydration level. The value of  $\beta$  obtained from the fits of  $\Gamma_1$  to Eq. 8 was found to be independent on hydration level within accuracy of simulations and equal  $0.33 \pm 0.01$  for both flexible and rigid lysozyme molecules. The values of the relaxation time  $\tau_1$ , obtained from the fitting of  $\Gamma_1$  to Eq. 8 with the stretching exponent  $\beta$  fixed at 0.33, are shown in Fig. 12. The value  $\tau_1$  continuously decreases with hydration (Fig. 13) and this decrease is much steeper at the surface of a rigid lysozyme, because of much slower rotational relaxation of water at low hydrations. The same trends are observed for the average relaxation time calculated as

$$\langle \tau_1 \rangle = \frac{\tau_1}{\beta} \Gamma\left(\frac{1}{\beta}\right), \quad (9)$$

with  $\Gamma$  as the gamma factorial function (see Tables 1 and 2).

The rotational relaxation may be also characterized by the second-rank correlation function  $\Gamma_2$ , which is directly related to the results of nuclear magnetic relaxation dispersion measurements. The second-rank correlation function  $\Gamma_2$  shows faster decay than  $\Gamma_1$ . Accordingly, the relaxation times  $\tau_1$  and  $\tau_2$  found from the fits of  $\Gamma_2$  to Eq. 8 are lower at all hydrations studied (see Fig. 13). The values of stretching exponent  $\beta$  derived from the fits of the second-rank correlation function to Eq. 8 were found independent on hydration and equal to  $\approx 0.245$  for the rigid and 0.225 for the flexible lysozyme molecules, respectively.

In contrast with the stretched exponential relaxation time, the Debye relaxation time  $\tau_2$  does not vary with hydration and stays at  $\tau_2 = 4.7 \pm 0.4$  ps and  $2.5 \pm 0.6$  ps for  $\Gamma_1$  and  $\Gamma_2$ , respectively (Fig. 13). The characteristic times of Debye relaxation of bulk TIP4P water molecules are 2.5 and 0.9 ps,

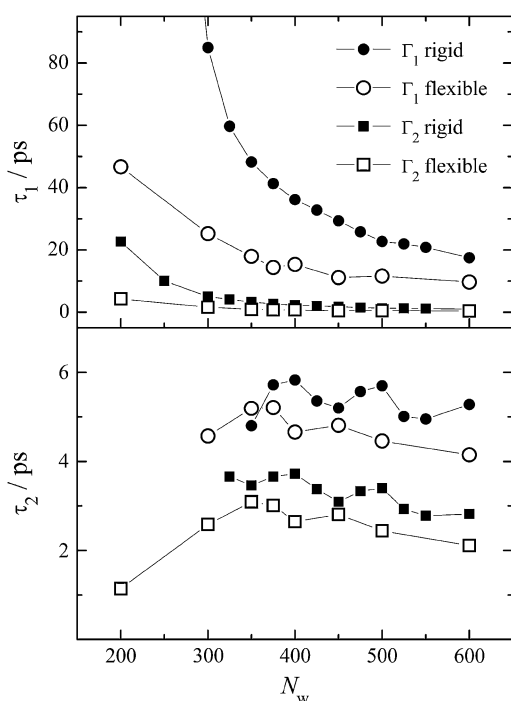


FIGURE 13 Relaxation times  $\tau_1$  and  $\tau_2$  found from the fits of Eq. 8 to the first-rank and second rank dipole-dipole autocorrelation functions  $\Gamma_1$  and  $\Gamma_2$  of water at the surface of flexible and rigid lysozyme molecules at various hydrations  $N_w$ .

respectively (90). The fraction  $a$  of water molecules with Debye-like rotational dynamics increases with hydration level, as it is shown in Fig. 14. At low hydrations,  $a$  is negligibly small and, therefore, cannot be estimated from the fits with a reasonable accuracy. At the surface of a rigid

**TABLE 1** Numbers of water molecules  $N_w$ , average number  $n_H$  of H-bonded neighbors, average relaxation time  $\langle\tau_1\rangle$  (ps) computed by Eq. 9, and relaxation time  $\tau_2$  (ps) of the first-rank and second-rank dipole-dipole correlation functions and their ratios for the rigid lysozyme molecule; the value of the stretching exponent  $\beta$  is 0.33 and 0.245 for  $\Gamma_1$  and  $\Gamma_2$ , respectively

$N_w$	$n_H$	$\langle\tau_1\rangle(\Gamma_1)$	$\langle\tau_1\rangle(\Gamma_2)$	$\langle\tau_1\rangle(\Gamma_1)/\langle\tau_1\rangle(\Gamma_2)$	$\tau_2(\Gamma_1)/\tau_2(\Gamma_2)$
200	1.55	6012	615	9.7	—
250	1.75	1370	274	5.0	—
300	1.91	528	138	3.8	—
325	1.98	371	112	3.3	—
350	2.05	300	90	3.3	1.4
375	2.11	257	75	3.5	1.6
400	2.16	225	63	3.6	1.6
425	2.20	204	55	3.7	1.6
450	2.25	182	48	3.8	1.7
475	2.30	160	41	3.9	1.7
500	2.34	141	35	4.1	1.7
525	2.38	136	34	4.1	1.7
550	2.42	129	32	4.0	1.8
600	2.47	108	26	4.1	1.9
Bulk		2.5	0.9	—	2.8

**TABLE 2** Numbers of water molecules  $N_w$ , average number of H-bonded neighbors  $n_H$ , average relaxation time  $\langle\tau_1\rangle$  (ps) computed by Eq. 9, and relaxation time  $\tau_2$  (ps) of the first-rank and second-rank dipole-dipole correlation functions and their ratios for the flexible lysozyme molecule; the value of the stretching exponent  $\beta$  is 0.33 and 0.245 for  $\Gamma_1$  and  $\Gamma_2$ , respectively

$N_w$	$n_H$	$\langle\tau_1\rangle(\Gamma_1)$	$\langle\tau_1\rangle(\Gamma_2)$	$\langle\tau_1\rangle(\Gamma_1)/\langle\tau_1\rangle(\Gamma_2)$	$\tau_2(\Gamma_1)/\tau_2(\Gamma_2)$
200	1.53	291	207	1.4	—
300	1.9	157	78	2.0	1.8
350	2.05	112	44	2.5	1.7
375	2.09	89	35	2.5	1.7
400	2.17	96	35	2.7	1.8
450	2.26	69	22	3.1	1.7
500	2.33	72	24	3.0	1.8
600	2.46	61	19	3.1	2.0
Bulk (90)		2.5	0.9	—	2.8

lysozyme, we have detected appearance of the water molecules with Debye-like rotational dynamics only when  $N_w > 300$ . At the flexible surface, such water molecules appear at much lower hydration (linear extrapolation of  $a(N_w)$  yields  $a = 0$  at  $N_w \approx 130$ ), and their fraction is  $\sim 20$ – $25\%$  at the percolation threshold (see Fig. 14).

## DISCUSSION

We have analyzed the effect of clustering on the dynamics of water molecules at the surface of low-hydrated lysozyme molecule. Character of water clustering drastically changes with increasing hydration and percolation analysis allows detail characterization of this process. Apart from various clustering properties (spanning probability, average cluster

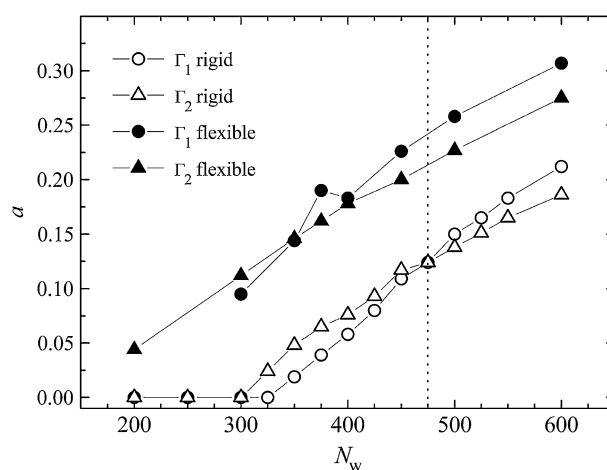


FIGURE 14 Amplitude  $a$  of the Debye term in Eq. 8, when it is fitted to the first-rank (circles) and second-rank (triangles) dipole-dipole autocorrelation functions  $\Gamma_1$  and  $\Gamma_2$  of water at the surface of flexible and rigid lysozymes at various hydrations  $N_w$ . Water percolation threshold is shown by the vertical dotted line.

size, etc.), it gives two specific hydration levels, which indicate important steps in the development of cluster structure: a midpoint of the percolation transition, where spanning water network exists with a probability of 50% and a true percolation threshold, where this network exists permanently (Fig. 2). These two hydrations characterize formation of a water monolayer at the surface of a biomolecule, because appearance of a spanning network should be identified with the first appearance of a water monolayer. Spanning water network at the percolation threshold is rarefied (its fractal dimension is  $\sim 1.9$ ), but covers a biomolecule homogeneously. Important functions of biomolecules appear in the hydration range, corresponding to the formation of a water monolayer via percolation transition (see Introduction). This justifies the importance of characterizing the dynamics of the hydrated biomolecule with respect to the characteristic hydration levels, mentioned above. Analysis of the translational and rotational dynamics of water molecules, done in this article, is the first step.

There are several factors, which determine translational motion of water molecules in such complex system as low-hydrated biomolecules: restriction of the motions in the direction normal to the protein surface; restriction of the motion due to the finite size of a biomolecule; spatial disorder due to the roughness and heterogeneity of the surface; and temporal disorder due to the presence of the strongly attractive sites at the surface. Importance of these factors depends on the time- and length scales considered, on the properties of a biomolecule, and on the hydration level. Localization of water molecules near the surface ultimately limits their displacements normal to the surface. Accordingly, the value of the diffusion coefficient, estimated from the time dependence of the total MSD, is essentially below the bulk value (Fig. 8). This apparent slowing-down of water motions reflects localization of molecules near a surface and does not necessarily mean decrease of their mobility at short timescale. Estimations of the diffusion coefficient of water, based on the MSD along the surface, are free from the confining effect of a surface and give values comparable to the values of the bulk. However, such comparison also has very relative character, as water diffusion is normal in the bulk case and anomalous at the surface of a biomolecule (Figs. 4–6).

Water mobility at the surface of a rigid lysozyme almost linearly increases with hydration level with only slight trend to saturation. This agrees with mainly linear dependence of water mobility on the hydration level at the surface of a rigid DNA molecule (57). Water-water interactions may be described by the average number  $n_H$  of H-bonded neighbors. For rigid lysozyme, the correlation of water mobility with  $n_H$  is linear for both short- and long-time mobility. Qualitative changes of the water clustering when approaching and crossing the percolation threshold does not affect this correlation noticeably. So, the water-water interactions is a dominant factor, which strongly facilitates water mobility at the surface of a rigid lysozyme with increasing hydration level.

Various characteristics of the short-time and long-time water mobility at the surface of a flexible lysozyme molecule (Figs. 7–9) show that they increase with hydration level and achieve saturation approximately at the percolation threshold. Above the midpoint of the percolation transition, water mobility linearly correlates with parameters, characterizing formation of a spanning water network (for example, with the average normalized size  $S_{av}^*$  of water clusters, Fig. 8). The correlation of water mobility with  $n_H$  is seen for the short- but not long-time mobility of water. Very small difference in the clustering and percolation transition of water at the surfaces of flexible and rigid lysozymes (Fig. 2) should not be responsible for the qualitative difference in the hydration dependence of water mobility. We may assume that dynamical motions of lysozyme facilitate faster rearrangement of water clusters, which makes water mobility more sensitive to the cluster structure. However, it is more reasonable to attribute specific hydration dependence of the water mobility at the surface of a flexible lysozyme molecule to its coupling with the dynamics of a lysozyme molecule.

Obviously, dynamics of a biomolecule and dynamics of its hydrations water should be coupled. For example, pressure-induced dynamic transition in crystalline Staphylococcal nuclease (SNase) causes similar qualitative changes of pressure dependence of the MSD of both water molecules and hydrogens of SNase molecule (93). So, comparison of water dynamics at rigid and flexible lysozyme may give insight on the dynamics of a lysozyme molecule. Correlation of water mobility with a presence of a spanning water network appears when lysozyme is flexible. The hydration-induced enhancement of lysozyme dynamics is maximal in the hydration range, bounded by the appearance of a spanning water network from below and by the percolation threshold from above. This picture agrees with the available experimental analysis of the effect of hydration on lysozyme dynamics (8,9,48,49,75,59). Namely, internal dynamics of lysozyme molecule is restored, when it is covered by some minimal amount of hydration water. Note that correlation between the percolation transition of water and pressure-induced dynamic transition of protein molecules was also observed in simulations of crystalline SNase (53).

The diffusion of water is anomalous at the surfaces of both rigid and flexible lysozymes. This behavior is observed in timescale from few picoseconds up to 100–200 ps. At longer timescale, the finite size of a lysozyme molecule leads to the saturation of water MSD, which is typical for translational diffusion in confined systems (94–96). The latter effect is noticeable in our simulations, when the total MSD exceeds  $\sim 1 \text{ nm}^2$ , that corresponds to the linear displacement on approximately half of the linear size of lysozyme. The anomalous diffusion of water near lysozyme surface in a wide range of hydrations is well described by the power law with exponent  $\alpha$  of  $\sim 0.78$ . Comparable values of the exponent  $\alpha$  were obtained for time dependence of the total MSD of hydration water in simulation studies of other

systems. For a fully hydrated plastocyanin, water in the layer of  $\sim 4$  to  $6$  Å width shows anomalous diffusion with  $\alpha$  of  $\sim 0.8$  (65,88). Comparable value of  $\alpha$  ( $\approx 0.6$ ) was observed in the first water layer near fully hydrated lysozyme (68). A slightly lower value of  $\alpha$  ( $\sim 0.5$ ) was obtained for translational motion of water in a low-hydrated silica pore (97) and larger ( $\sim 0.8$ ) for water diffusion in the surface layer of a completely filled nanopore (98).

Whereas we obtained  $\alpha$  of  $\sim 0.78$  from the time dependence of the total MSD, the time behavior of the MSD parallel to the surface is described by  $\alpha \sim 0.40$  (see Fig. 5), which is surprisingly close to the experimental value of  $\alpha$  for water diffusion at the surface of a low-hydrated myoglobin molecule (87). The lower values of  $\alpha$  for parallel MSD should be attributed to the stronger spatial disorder for the two-dimensional motions in a plane in comparison with the motions in a layer of some finite width. Note, that  $\alpha$  in the surface water layer found from the simulations of fully hydrated systems strongly depends on the definition of hydration layer (65,88). In contrast, in partially hydrated lysozyme we have found  $\alpha$  to be almost independent on hydration level. This behavior can be expected, when anomalous diffusion is caused mainly by the spatial disorder. Presence of a strongly adsorbing sites at lysozyme surface (45,46), which provide long residence times for water molecules, affects time dependence of the MSD at short times only and decreases the effective value of  $\alpha$  at this timescale. At low hydrations, it can be approximately taken into account by adding some constant to the time dependence of the MSD (see Eqs. 3 and 4). This effect quickly disappears with increasing hydration level, because the contribution to MSD from strongly bound molecules becomes progressively less important. Assuming the anomalous diffusion of water to be induced only by spatial disorder of the protein surface,  $\alpha = d_s/d_s^f$ , where  $d_s^f$  is the fractal dimension of the protein surface ( $d_s^f \sim 2.2$  (66)) and  $d_s$  is a spectral dimension. Our simulations yield  $d_s \approx 1.74$  and  $1.70$  for the rigid and flexible lysozyme molecules, respectively.

We observed a strong retardation of the rotational motion of water near lysozyme, which achieves approximately two orders of the magnitude at the lowest hydration level studied (see Tables 1 and 2 and Fig. 13). At low hydrations, rotational dynamics of water shows stretched exponential relaxation with broad distribution of relaxation times described by the stretched exponent  $\beta \approx 0.33$  for the first rank and even smaller  $\beta \approx 0.23$  for the second-rank dipole-dipole correlation functions. The water molecules with strong retardation of rotational motion and with broad distribution of relaxation times should be considered as strongly bound. The similar low values of the stretching exponent were observed in a neutron scattering experiment for combined rotational-translational motion of water in hydrated myoglobin ( $\beta \approx 0.3$ ) (87) and in simulations of water near mica surface ( $\beta \approx 0.25$ ) (99). Contrary to the previous studies of water rotational motions near biomolecules (68,88), we observe also weakly

bound water molecules with Debye rotational relaxation. These water molecules show fast rotational motion with relaxation times  $\tau_2 \approx 4.7$  and  $2.5$  ps for the first and second-rank autocorrelation functions, respectively, which are noticeably larger the bulk values ( $2.5$  and  $0.9$  ps (90)). So, in a wide hydration range, rotational motions of water molecules can be well described by the two-term Eq. 8. Independence of the stretched exponent  $\beta$  and the value of  $\tau_2$  on the hydration level evidences in favor of such description.

The mechanism of rotational dynamics affects the ratio of the relaxation times derived from  $\Gamma_1$  and  $\Gamma_2$ . This ratio is 3 for the isotropic rotational diffusion and is essentially lower for reorientations, which involve large-amplitude angular jumps (100). In the case of a flexible lysozyme, the ratio  $\langle \tau_1 \rangle(\Gamma_1)/\langle \tau_1 \rangle(\Gamma_2)$  for the stretched exponential relaxation increases upon hydration and achieves the value of  $\sim 3$  at monolayer coverage (Table 2). Rather different behavior of  $\langle \tau_1 \rangle(\Gamma_1)/\langle \tau_1 \rangle(\Gamma_2)$  is seen at the surface of a rigid lysozyme, where this ratio always exceeds 3 and becomes higher at low hydrations (Table 1). The ratio  $\tau_2(\Gamma_1)/\tau_2(\Gamma_2)$  for weakly bound water varies slowly with hydration level and does not exceed 2 even at monolayer coverage (Tables 1 and 2). The ratio of  $\sim 2$  was obtained for  $4$  Å thick water layer near fully hydrated plastocyanin (88). Low values of the ratio  $\tau_2(\Gamma_1)/\tau_2(\Gamma_2)$  indicates that reorientation mechanism of weakly bound water involves large-amplitude angular jumps rather than small diffusive steps (100).

Rotational motion of hydration water affects the dielectric properties of hydrated lysozyme (44,45,101,102). The dielectric increment  $\Delta\epsilon$ , originated from the reorientation of dipole moments  $\mu$  in presence of external electric field, may be estimated as (101,103)

$$\Delta\epsilon = \frac{\rho_w \mu^2}{2\epsilon_0 kT} g, \quad (10)$$

where  $\rho_w$  is the number density of dipoles;  $\epsilon_0$  is the permittivity of free space;  $k$  is the Boltzmann constant; and  $g$  is the Kirkwood factor, which accounts for correlations in dipole orientations. We may use Eq. 10 to estimate  $\Delta\epsilon$  caused by rotation of water molecules in low hydrated systems assuming  $\mu$  to be equal to the dipole moment in a vapor phase and using  $\rho_w$  from simulations of a model lysozyme powder (50). At a given frequency  $\nu$  of external electric field, only dipoles with relaxation times  $< 1/(2\pi\nu)$  contribute to  $\Delta\epsilon$ , and  $\rho_w$  in Eq. 10 is a density of water molecules with  $\tau < 1/(2\pi\nu)$ . Dielectric studies of a lysozyme powder show that 32 water molecules per one lysozyme have relaxation times  $\tau > 10^4$  ns and should be considered as irrotationally bound at  $\nu = 10$  kHz (45, 102). In a model powder with the density  $0.66$  g  $\text{cm}^{-3}$  at zero hydration (50), the density of water molecules, which should contribute to  $\Delta\epsilon$  at  $\nu = 10$  kHz, is  $\rho_w = (N_w - 32)/36$  ( $\text{nm}^{-3}$ ), where  $N_w$  is a number of water molecules per one lysozyme. Hydration dependence of the dielectric increment  $\Delta\epsilon$  (10 kHz) for a model lysozyme powder,

calculated by Eq. 10 in absence of the correlation of dipoles ( $g = 1$ ), is shown in Fig. 15 (*left panel*). This dependence may be compared with  $\Delta\epsilon$  measured as a difference of  $\epsilon$  at  $\nu = 10$  kHz and 9.95 GHz (45), when experimental data are shifted to account for contribution of lysozyme polarization at zero hydration. There is a good agreement between simulated and experimental data up to  $h \sim 0.12$  g/g. With approaching the percolation threshold (at  $h \approx 0.14$  g/g (17)), growth of water clusters and formation of a spanning water network lead to increasing correlation of water dipoles ( $g > 1$ ) and experimental  $\Delta\epsilon$  starts to increase faster upon hydration. Above the percolation threshold, where the spanning network of hydration water exists permanently, a slope of the dependence  $\Delta\epsilon(h)$  is  $\sim 3$  times larger than at low hydrations. This value is comparable with the Kirkwood factor  $g = 2.9$  for a bulk liquid water (103).

Dielectric increment of hydrated lysozyme powder measured at  $\nu = 25$  GHz (44), arises from reorientation of water molecules with relaxation times  $< 6.4$  ps, which may be related to the weakly bound water molecules found in our simulations. To compare the experimental and simulation data in this case, we have to establish the relation between the hydration level of a single lysozyme molecule and the hydration level of a powder. Water dynamics, as well as water clustering, is very sensitive to the number  $n_H$  of water-water hydrogen bonds (56). Therefore, it is reasonable to consider the states of hydration water with the same value of  $n_H$  as similar. In Fig. 16 we show  $n_H$  of water at the surface of a single lysozyme molecule and  $n_H$  of water in the model lysozyme powder (50) as functions of  $N_w$  and hydration  $h$ .

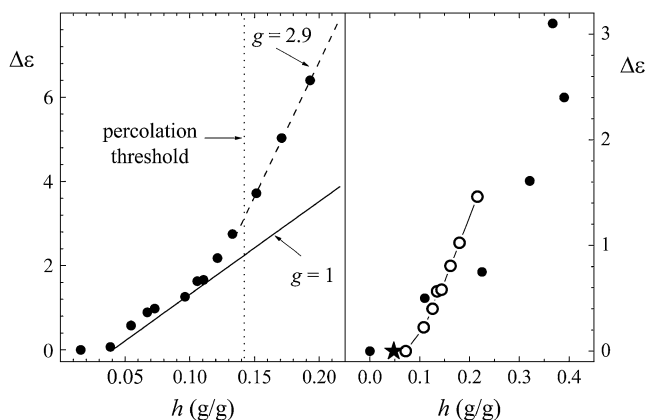


FIGURE 15 (*Left panel*) Dielectric increment  $\Delta\epsilon$  calculated with Eq. 10, taking into account strongly and weakly bound water and excluding the irrotationally bound water (solid line). Experimental data from Bone and Pethig (45) corrected on lysozyme contribution at zero hydration (solid circles). The slope, corresponding to Kirkwood factor  $g = 2.9$ , is shown by dashed line. The percolation threshold of water (17) is shown by dotted line. (*Right panel*) Contribution to  $\Delta\epsilon$  from weakly bound water molecules calculated with Eq. 10 (open circles) and experimental data at  $\nu = 25$  GHz from Harvey and Hoekstra (44) corrected on lysozyme contribution at zero hydration (solid circles). Appearance of weakly bound water molecules upon hydration is indicated by star.

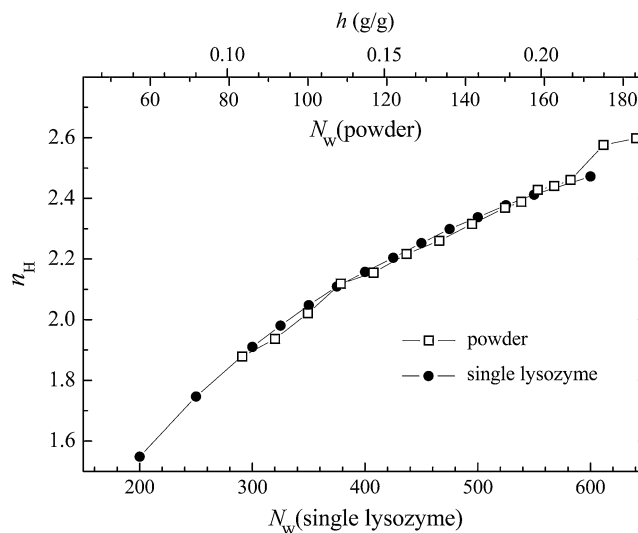


FIGURE 16 Average number of water-water hydrogen bonds at the surface of a flexible lysozyme molecule and in the rigid lysozyme powder shown as functions of  $N_w$  and  $h$ .

Both  $n_H$  dependences coincide in a wide hydration range, when  $N_w$  for a single lysozyme molecule is scaled by a factor  $2/7$ . Contribution of weakly bound water molecules to dielectric increment  $\Delta\epsilon$  of a model lysozyme powder was calculated by Eq. 10, taking into account their fraction  $a$  (Fig. 14) and assuming  $g = 1$ . The calculated  $\Delta\epsilon$  values at various hydrations (*open symbols* in the *right panel* of Fig. 15) may be compared with the experimental data at  $\nu = 25$  GHz (44) corrected for contribution of lysozyme polarization at zero hydration (*solid symbols* in the *right panel* of Fig. 15). A good agreement of experimental and simulation data in this case cannot be expected, because  $\Delta\epsilon$  measured at  $\nu = 25$  GHz should contain contribution only from a part of weakly bound water (from molecules with  $\tau < \sim 6$  ps). Besides, at  $h > 0.3$ , the experimental data (44) should contain contribution from bulklike water molecules that appear after completion of the first monolayer (49). Note finally that weakly bound water molecules appear at  $N_w \approx 130$ , which corresponds to  $h \approx 0.05$  in the case of a powder (*star* in the *right panel* of Fig. 15); that is, just after the strongly adsorptive sites of lysozyme are saturated at  $h \approx 0.04$  (45,49).

We thank Deutschen Forschungsgemeinschaft (Forschergruppe grant No. 436) for financial support.

## REFERENCES

- Chaplin, M. 2006. Do we underestimate the importance of water in cell biology? *Nat. Rev. Mol. Cell Biol.* 7:861–866.
- Levy, Y., and J. N. Onuchic. 2006. Water mediation in protein folding and molecular recognition. *Annu. Rev. Biophys. Biomol. Struct.* 35:389–415.
- Helms, V. 2007. Protein dynamics tightly connected to the dynamics of surrounding and internal water molecules. *Chem. Phys. Chem.* 8:23–33.

4. Clegg, J. S. 1974. Interrelationships between water and metabolism in *Artemia salina* cysts: hydration-dehydration from the liquid and vapor phases. *J. Exp. Biol.* 61:291–308.
5. Vertucci, C. W., and A. C. Leopold. 1987. Oxidative processes in soybean and pea seeds. *Plant Physiol.* 84:1038–1043.
6. Stevens, E., and L. Stevens. 1979. The effect of restricted hydration on the rate of reaction of glucose 6-phosphate dehydrogenase, phosphoglucose isomerase, hexokinase and fumarase. *Biochem. J.* 179:161–167.
7. Rupley, J. A., P.-H. Yang, and G. Tollin. 1980. Thermodynamic and related studies of water interacting with proteins. In *Water in Polymers*. ACS Symposium Series, Vol. 127. S. P. Rouland, editor. American Chemical Society, Washington, DC.
8. Rupley, J. A., E. Gratton, and G. Careri. 1983. Water and globular proteins. *Trends Biochem. Sci.* 8:18–22.
9. Schinkel, J. E., N. W. Downer, and J. A. Rupley. 1985. Hydrogen exchange of lysozyme powders. Hydration dependence of internal motions. *Biochemistry.* 24:352–366.
10. Yang, F., and A. J. Russel. 2000. The role of hydration in enzyme activity and stability. 2. Alcohol dehydrogenase activity and stability in a continuous gas phase reactor. *Biotechnol. Bioeng.* 49:709–716.
11. Lind, P. A., R. M. Daniel, C. Monk, and R. V. Dunn. 2004. Esterase catalysis of substrate vapor: enzyme activity occurs at very low hydration. *Biochim. Biophys. Acta.* 1702:103–110.
12. Halling, P. J. 2004. What can we learn by studying enzymes in non-aqueous media? *Philos. Trans. R. Soc. Lond. B Biol. Sci.* 359:1287–1297.
13. Fitter, J., S. A. W. Verclas, R. E. Lechner, and N. A. Dencher. 1998. Function and picosecond dynamics of bacteriorhodopsin in purple membrane at different lipidation and hydration. *FEBS Lett.* 433:321–325.
14. Korenstein, R., and B. Hess. 1977. Hydration effects on *cis-trans* isomerization of bacteriorhodopsin. *FEBS Lett.* 82:7–11.
15. Varo, G., and L. Keszthelyi. 1983. Photoelectric signals from dried oriented purple membranes of *Halobacterium halobium*. *Biophys. J.* 43:47–51.
16. Saenger, W. 1984. *Principles of Nucleic Acid Structure*. Springer-Verlag, New York.
17. Careri, G., A. Giansanti, and J. A. Rupley. 1988. Critical exponents of protonic percolation in hydrated lysozyme powders. *Phys. Rev. A.* 37:2703–2705.
18. Pizzitutti, F., and F. Bruni. 2001. Glassy dynamics and enzymatic activity of lysozyme. *Phys. Rev. E.* 64:052905.
19. Bruni, F., G. Careri, and A. C. Leopold. 1989. Critical exponents of protonic percolation in maize seeds. *Phys. Rev. A.* 40:2803–2805.
20. Konsta, A. A., J. Laudat, and P. Pissis. 1997. Dielectric investigation of the protonic conductivity in plant seeds. *Solid State Ionics.* 97:97–104.
21. Sokolowska, D., A. Krol-Otwinowska, and J. K. Moscicki. 2004. Water-network percolation transitions in hydrated yeast. *Phys. Rev. E.* 70:052901.
22. Bruni, F., G. Careri, and J. S. Clegg. 1990. Dielectric properties of *Artemia* cysts at low water contents. Evidence for a percolative transition. *Biophys. J.* 23:932–939.
23. Rupley, J. A., L. Siemankowski, G. Careri, and F. Bruni. 1988. Two-dimensional protonic percolation on lightly hydrated purple membrane. *Proc. Natl. Acad. Sci. USA.* 85:9022–9025.
24. Careri, G., A. Giansanti, and J. A. Rupley. 1986. Proton percolation on hydrated lysozyme powders. *Proc. Natl. Acad. Sci. USA.* 83:6810–6814.
25. Haranczyk, H. 2003. *On Water in Extremely Dry Biological Systems*. Jagiellonian University Press, Krakow, Poland.
26. Rasmussen, B. F., A. M. Stock, D. Ringe, and G. A. Petsco. 1992. Crystalline ribonuclease A loses function below the dynamic transition at 220K. *Nature.* 357:423–424.
27. Lichtenegger, H., W. Doster, T. Kleinert, A. Birk, B. Sepiol, and G. Vogl. 1999. Heme-solvent coupling: a Mössbauer study of myoglobin in sucrose. *Biophys. J.* 76:414–422.
28. Ferrand, M., A. J. Dianoux, W. Petry, and G. Zaccai. 1993. Thermal motions and function of bacteriorhodopsin in purple membranes: effect of temperature and hydration studied by neutron scattering. *Proc. Natl. Acad. Sci. USA.* 90:9668–9672.
29. Fitter, J. 1999. The temperature dependence of internal molecular motion in hydrated and dry  $\alpha$ -amylase: the role of hydration water in the dynamical transition of proteins. *Biophys. J.* 76:1034–1042.
30. Paciaroni, A., S. Cinemmi, and G. Onori. 2002. Effect of the environment on the protein dynamic transition: a neutron scattering study. *Biophys. J.* 83:1157–1164.
31. Tarek, M., and D. J. Tobias. 2002. Role of protein-water hydrogen bond dynamics in the protein dynamical transition. *Phys. Rev. Lett.* 88:138101.
32. Tournier, A. L., and J. C. Smith. 2003. Principal components of the protein dynamical transition. *Phys. Rev. Lett.* 91:208106.
33. Tournier, A. L., J. Xu, and J. C. Smith. 2003. Translational hydration water dynamics drives the protein glass transition. *Biophys. J.* 85:1871–1875.
34. Caliskan, G., R. Briber, D. Thirumalai, V. Garcia-Sakai, S. Woodson, and A. Sokolov. 2006. Dynamic transition in tRNA is solvent induced. *J. Am. Chem. Soc.* 128:32–33.
35. Faraone, A., L. Liu, C.-Y. Mou, C.-W. Yen, and S.-H. Chen. 2004. Fragile-to-strong liquid transition in deeply supercooled confined water. *J. Chem. Phys.* 121:10843–10846.
36. Liu, L., S.-H. Chen, A. Faraone, C.-W. Yen, and C.-Y. Mou. 2005. Pressure dependence of fragile-to-strong transition and a possible second critical point in supercooled confined water. *Phys. Rev. Lett.* 95:117802.
37. Chen, S.-H., L. Liu, X. Chu, Y. Zhang, E. Fratini, P. Baglioni, A. Faraone, and E. Mamontov. 2006. Experimental evidence of fragile-to-strong dynamic crossover in DNA hydration water. *J. Chem. Phys.* 125:171103.
38. Chen, S.-H., L. Liu, E. Fratini, P. Baglioni, A. Faraone, and E. Mamontov. 2006. Observation of fragile-to-strong dynamic crossover in protein hydration water. *Proc. Natl. Acad. Sci. USA.* 103:9012–9016.
39. Xu, L., P. Kumar, S. V. Buldyrev, S.-H. Chen, P. H. Poole, F. Sciortino, and H. E. Stanley. 2005. Relation between the Widom line and the dynamic crossover in systems with a liquid-liquid phase transition. *Proc. Natl. Acad. Sci. USA.* 102:16558–16562.
40. Frauenfelder, H., G. A. Pestko, and D. Tsemoglou. 1979. Temperature-dependent x-ray diffraction as a probe of protein structural dynamics. *Nature.* 280:558–563.
41. Szent-Gyorgyi, A. 1941. The study of energy-levels in biochemistry. *Nature.* 3745:157–159.
42. Gascoyne, P. R., R. Pethig, and A. Szent-Gyorgyi. 1981. Water structure-dependent charge transport in proteins. *Proc. Natl. Acad. Sci. USA.* 78:261–265.
43. Rosen, D. 1963. Dielectric properties of protein powders with adsorbed water. *Trans. Faraday Soc.* 59:2178–2191.
44. Harvey, S. C., and P. Hoekstra. 1972. Dielectric relaxation spectra of water adsorbed at lysozyme. *J. Phys. Chem.* 76:2987–2994.
45. Bone, S., and R. Pethig. 1982. Dielectric studies of the binding of water to lysozyme. *J. Mol. Biol.* 157:571–575.
46. Bone, S., and R. Pethig. 1985. Dielectric studies of protein hydration and hydration-induced flexibility. *J. Mol. Biol.* 181:323–326.
47. Careri, G., M. Geraci, A. Giansanti, and J. A. Rupley. 1985. Protonic conductivity of hydrated lysozyme powders at megahertz frequencies. *Proc. Natl. Acad. Sci. USA.* 82:5342–5346.
48. Yang, P.-H., and J. A. Rupley. 1979. Protein-water interactions. Heat capacity of the lysozyme-water system. *Biochemistry.* 18:2654–2661.
49. Rupley, J. A., and G. Careri. 1991. Protein hydration and function. *Adv. Protein Chem.* 41:37–172.

50. Oleinikova, A., N. Smolin, I. Brovchenko, A. Geiger, and R. Winter. 2005. Formation of spanning water networks on protein surfaces via 2D percolation transition. *J. Phys. Chem. B*. 109:1988–1998.
51. Oleinikova, A., I. Brovchenko, N. Smolin, A. Krukau, A. Geiger, and R. Winter. 2005. Percolation transition of hydration water: from planar hydrophilic surfaces to proteins. *Phys. Rev. Lett.* 95:247802.
52. Brovchenko, I., A. Krukau, N. Smolin, A. Oleinikova, A. Geiger, and R. Winter. 2005. Thermal breaking of spanning water networks in the hydration shell of proteins. *J. Chem. Phys.* 123:224905.
53. Oleinikova, A., N. Smolin, and I. Brovchenko. 2006. Origin of the dynamic transition upon pressurization of crystalline proteins. *J. Phys. Chem. B*. 110:19619–19624.
54. Smolin, N., A. Oleinikova, I. Brovchenko, A. Geiger, and R. Winter. 2005. Properties of spanning water networks at protein surfaces. *J. Phys. Chem. B*. 109:10995–11005.
55. Oleinikova, A., I. Brovchenko, and A. Geiger. 2006. Percolation transition of hydration water at hydrophilic surfaces. *Physica A*. 364:1–12.
56. Oleinikova, A., and I. Brovchenko. 2006. Percolation transition of hydration water in biosystems. *Mol. Phys.* 104:3841–3855.
57. Brovchenko, I., A. Krukau, A. Oleinikova, and A. K. Mazur. 2006. Water percolation governs polymorphic transitions and conductivity of DNA. *Phys. Rev. Lett.* 97:137801.
58. Brovchenko, I., and A. Oleinikova. 2006. Molecular organization of gases and liquids at solid surfaces. In *Handbook of Theoretical and Computational Nanotechnology*, Vol. 9, Chapt. 3. American Scientific Publishers, Stevenson Ranch, CA.
59. Roh, J. H., J. E. Curtis, S. Azzam, V. N. Novikov, I. Peral, Z. Chowdhuri, R. B. Gregory, and A. P. Sokolov. 2006. Influence of hydration on the dynamics of lysozyme. *Biophys. J.* 91:2573–2588.
60. Lehnert, U., V. Reat, M. Weik, G. Zaccai, and C. Pfister. 1998. Thermal motion of bacteriorhodopsin at different hydration levels. *Biophys. J.* 75:1945–1952.
61. Bellissent-Funel, M.-C., J.-M. Zanotti, and S. H. Chen. 1996. Slow dynamics of water molecules on the surface of a globular protein. *Faraday Discuss.* 103:281–294.
62. Dellerue, S., and M.-C. Bellissent-Funel. 2000. Relaxational dynamics of water molecules at protein surface. *Chem. Phys.* 258:315–325.
63. Russo, D., R. Murarka, G. Hura, E. Verschell, J. Copley, and T. Head-Gordon. 2004. Evidence for anomalous hydration dynamics near a model hydrophobic peptide. *J. Phys. Chem. B*. 108:19885–19893.
64. Bon, C., A. J. Dianoux, M. Ferrand, and M. S. Lehmann. 2002. A model for water motion in crystals of lysozyme based on an incoherent quasielastic neutron-scattering study. *Biophys. J.* 83:1578–1588.
65. Bizzarri, A., and S. Cannistraro. 1996. Molecular dynamics simulation evidence of anomalous diffusion of protein hydration water. *Phys. Rev. E*. 53:R3040–R3043.
66. Bizzarri, A., C. Rocchi, and S. Cannistraro. 1996. Origin of the anomalous diffusion observed by MD simulation at the protein-water interface. *Chem. Phys. Lett.* 263:559–566.
67. Tarek, M., and D. Tobias. 2000. The dynamics of protein hydration water: a quantitative comparison of molecular dynamic simulations and neutron-scattering experiments. *Biophys. J.* 79:3244–3275.
68. Marchi, M., F. Sterpone, and M. Ceccarelli. 2002. Water rotational relaxation and diffusion in hydrated lysozyme. *J. Am. Chem. Soc.* 124:6787–6791.
69. Careri, G., A. Giansanti, and E. Gratton. 1979. Lysozyme film hydration events: an IR and gravimetric study. *Biopolymers*. 18:1187–1203.
70. Pissis, P., and A. Anagnostopoulou-Konsta. 1990. Protonic percolation on hydrated lysozyme powders studied by the method of thermally stimulated depolarization currents. *J. Phys. D: Appl. Phys.* 23:932–939.
71. Urabe, H., Y. Sugawara, M. Ataka, and A. Rupprecht. 1998. Low-frequency Raman spectra of lysozyme crystals and oriented DNA films: dynamics of crystal water. *Biophys. J.* 74:1533–1540.
72. Suhrman, P. M., and G. Smith. 2003. A percolation transition cluster model of the temperature dependent dielectric properties of hydrated proteins. *J. Phys. D: Appl. Phys.* 36:336–342.
73. Cinelli, S., A. D. Francesco, G. Onori, and A. Paciaroni. 2004. Thermal stability and internal dynamics of lysozyme as affected by hydration. *Phys. Chem. Chem. Phys.* 6:3591–3595.
74. Knab, J., J.-Y. Chen, and A. Markelz. 2006. Hydration dependence of conformational dielectric relaxation of lysozyme. *Biophys. J.* 90:2576–2581.
75. Roh, J. H., V. N. Novikov, R. B. Gregory, J. E. Curtis, Z. Chowdhuri, and A. P. Sokolov. 2005. Onsets of anharmonicity in protein dynamics. *Phys. Rev. Lett.* 95:038101.
76. Cinelli, S., M. Freda, G. Onori, A. Paciaroni, and A. Santucci. 2005. Hydration-dependent internal dynamics of macromolecules: a neutron scattering study. *J. Mol. Liquids*. 117:99–105.
77. McKenzie, H. A., and F. H. J. White. 1991. Lysozyme and A-lactalbumin: structure, function and interrelationships. *Adv. Protein Chem.* 41:174–315.
78. Berman, H. M., J. Westbrook, Z. Feng, G. Gilliland, T. N. Bhat, H. Weissig, I. N. Shindyalov, and P. E. Bourne. 2000. The Protein Data Bank. *Nucleic Acids Res.* 28:235–242.
79. Kundrot, C. E., and F. M. Richards. 1987. Crystal structure of hen egg-white lysozyme at a hydrostatic pressure of 1000 atmospheres. *J. Mol. Biol.* 193:157–170.
80. Cornell, W. D., P. Cieplak, C. I. Bayly, I. R. Gould, K. M. Merz, D. M. Ferguson, D. C. Spellmeyer, T. Fox, J. W. Caldwell, and P. A. Kollman. 1995. A second generation force field for the simulation of proteins, nucleic acids, and organic molecules. *J. Am. Chem. Soc.* 117:5179–5197.
81. Jorgensen, W. L., J. Chandrasekhar, J. D. Madura, R. W. Impey, and M. L. Klein. 1983. Comparison of simple potential functions for simulating liquid water. *J. Chem. Phys.* 79:926–935.
82. Essmann, U., L. Perera, M. L. Berkowitz, T. Darden, H. Lee, and L. G. Pedersen. 1995. A smooth particle mesh Ewald method. *J. Chem. Phys.* 103:8577–8593.
83. Berendsen, H. J. C., J. P. M. Postma, W. F. van Gunsteren, A. DiNola, and J. R. Haak. 1984. Molecular dynamics with coupling to an external bath. *J. Chem. Phys.* 81:3684–3690.
84. Nose, S. 1984. A molecular dynamics method for simulations in the canonical ensemble. *Mol. Phys.* 52:255–268.
85. Hoover, W. G. 1985. Canonical dynamics: equilibrium phase-space distributions. *Phys. Rev. A*. 31:1695–1697.
86. Stauffer, D. 1985. *Introduction to Percolation Theory*. Taylor and Francis, London; Bristol, PA.
87. Settles, M., and W. Doster. 1996. Anomalous diffusion of the adsorbed water: a neutron scattering study of hydrated myoglobin. *Faraday Discuss.* 103:269–279.
88. Rocchi, C., A. R. Bizzarri, and S. Cannistraro. 1998. Water dynamical anomalies evidences by molecular dynamics simulations at the solvent-protein. *Phys. Rev. E*. 57:3315–3325.
89. Makarov, V. A., M. Feig, B. K. Andrews, and B. M. Pettitt. 1998. Diffusion of solvent around biomolecular solutes: a molecular dynamics simulation study. *Biophys. J.* 75:150–158.
90. van der Spoel, D., P. J. van Maaren, and H. J. C. Berendsen. 1998. A systematic study of water models for molecular simulation: derivation of water models optimized for use with a reaction field. *J. Chem. Phys.* 108:10220–10230.
91. Kohlrausch, R. 1854. Theory of the electrical residue in the Leiden bottle. *Pogg. Ann. Phys. Chem.* 91:179–214.
92. Williams, G., and D. C. Watts. 1970. Non-symmetrical dielectric relaxation behavior arising from a simple empirical decay function. *Trans. Faraday Soc.* 66:80–85.
93. Meinhold, L., and J. C. Smith. 2005. Pressure-dependent transition in protein dynamics at about 4 kbar revealed by molecular dynamics simulation. *Phys. Rev. E*. 72:061908.

94. Schoen, M., J. H. Cushman, D. J. Diestler, and C. L. Rhykerd, Jr. 1988. Fluids in micro-pores. II. Self-diffusion in a simple classical fluid in a slit pore. *J. Chem. Phys.* 88:1394–1406.
95. Brovchenko, I., A. Geiger, A. Oleinikova, and D. Paschek. 2003. Phase coexistence and dynamic properties of water in nanopores. *Eur. Phys. J. E.* 12:69–76.
96. Sega, M., R. Vallauri, and S. Melchionna. 2005. Diffusion of water in confined geometry: the case of a multilamellar bilayer. *Phys. Rev. E.* 72:041201.
97. Gallo, P., and M. Rovere. 2003. Anomalous dynamics of confined water at low hydration. *J. Phys.: Condens. Matter.* 15:7625–7633.
98. Malek, K., T. Odijk, and M.-O. Coppens. 2005. Diffusion of water and sodium counterions in nanopores of a  $\beta$ -lactoglobulin crystal: a molecular dynamics study. *Nanotechnology.* 16:S522–S530.
99. Leng, Y., and P. T. Cummings. 2005. Fluidity of hydration layers nanoconfined between mica surfaces. *Phys. Rev. Lett.* 94:026101.
100. Laage, D., and J. T. Hynes. 2006. A molecular jump mechanism of water reorientation. *Science.* 311:832–835.
101. Pethig, R. 1992. Protein-water interactions determined by dielectric methods. *Annu. Rev. Phys. Chem.* 43:177–205.
102. Bone, S. 1996. Dielectric and gravimetric studied of water binding to lysozyme. *Phys. Med. Biol.* 41:1265–1275.
103. Kirkwood, J. G. 1939. The dielectric polarization of polar liquids. *J. Chem. Phys.* 7:911–919.